JACS
JOURNAL OF THE AMERICAN CHEMICAL SOCIETY
Communication
pubs.acs.org/JACS

Heavily n-Dopable π-Conjugated Redox Polymers with Ultrafast Energy Storage Capability

Yanliang Liang,[†] Zhihua Chen,[§] Yan Jing,[†] Yaoguang Rong,[†] Antonio Facchetti,*[,§] and Yan Yao*[,†,‡]

[†]Department of Electrical and Computer Engineering and [‡]Texas Center for Superconductivity, University of Houston, Houston, Texas 77204, United States

[§]Polyera Corporation, 8045 Lamon Avenue, Skokie, Illinois 60077, United States

Supporting Information

ABSTRACT: We report here the first successful demonstration of a "π-conjugated redox polymer" simultaneously featuring a π-conjugated backbone and integrated redox sites, which can be stably and reversibly n-doped to a high doping level of 2.0 with significantly enhanced electronic conductivity. The properties of such a heavily n-dopable polymer, poly{[*N*,*N*′-bis(2-octyldodecyl)-1,4,5,8-naphthalenedicarboximide-2,6-diyl]-*alt*-5,5′-(2,2′-bithiophene)} (P(NDI2OD-T2)), were compared *vis-à-vis* to those of the corresponding backbone-insulated poly{[*N*,*N*′-bis(2-octyldodecyl)-1,4,5,8-naphthalenedicarboximide-2,6-diyl]-*alt*-5,5′-[2,2′-(1,2-ethanediyl)bithiophene]} (P(NDI2OD-TET)). When evaluated as a charge storage material for rechargeable Li batteries, P(NDI2OD-T2) delivers 95% of its theoretical capacity at a high rate of 100C (72 s per charge−discharge cycle) under practical measurement conditions as well as 96% capacity retention after 3000 cycles of deep discharge−charge. Electrochemical, impedance, and charge-transport measurements unambiguously demonstrate that the ultrafast electrode kinetics of P(NDI2OD-T2) are attributed to the high electronic conductivity of the polymer in the heavily n-doped state.

Organic π-conjugated polymers are emerging as a materials class for energy-related applications enabling a path to a more sustainable energy landscape without the need of energy-intensive, expensive, and sometimes toxic metal-based compounds.[1] Furthermore, the possibility to fabricate lightweight and mechanically flexible devices makes polymeric materials even more attractive. Hole-transporting (semi)conducting polymers with substantial redox activity and electronic conductivity have been long recognized as electrode materials for batteries, supercapacitors, and thermoelectrics.[2] However, all-polymer devices of this type have been difficult to realize due to the limitations of electron-transporting polymers.[3] Two general classes of electron-transporting polymers are known: π-conjugated polymers and nonconjugated redox polymers.[2a] Electron-transporting (or n-type) π-conjugated polymers typically need multiple repeating units in the backbone to stabilize injected electrons. Thus, the inability to stably and reversibly store these charges limits the n-doping level,[4] which in turn reduces the amount of free electrons and therefore restricts the electronic conductivity. On the other hand, nonconjugated redox polymers have dedicated redox active sites accepting one or more electrons per repeating unit[5] but lack a π-conjugated backbone as found in π-conjugated polymers, which is crucial for efficient electron conduction. Since the advantages of the two classes of polymers perfectly complement each other, the weakness of both polymers could be addressed by a rational combination of the characteristics from each class, such as a "π-conjugated redox polymer" (Figure 1a). Pioneering attempts to construct such a polymer

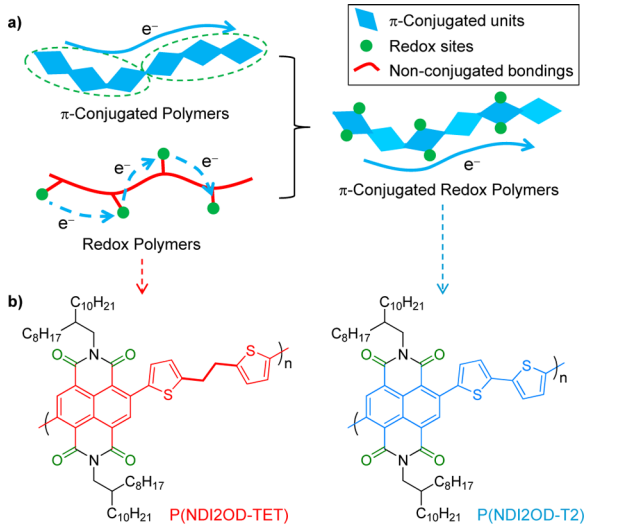

Figure 1. (a) Graphical illustration of the structural characteristics of π-conjugated polymers, redox polymers, and π-conjugated redox polymers. (b) Molecular structure of the nonconjugated P(NDI2OD-TET) and the π-conjugated P(NDI2OD-T2).

were limited by insufficient reversibility of the doping process,[6] unknown doping level,[6b,c,7] and/or uninvestigated/poor conductivity of the n-doped state.[6,7] Thus, it remains a major challenge to develop heavily n-dopable π-conjugated polymers with high electronic conductivity.

Herein we report the first demonstration of a π-conjugated redox polymer in poly{[*N*,*N*′-bis(2-octyldodecyl)-1,4,5,8-naphthalenedicarboximide-2,6-diyl]-*alt*-5,5′-(2,2′-bithiophene)} (P(NDI2OD-T2)), which can be stably and reversibly n-doped to a high doping level (2.0) and exhibits significant electronic

Received: March 6, 2015
Published: March 31, 2015

DOI: 10.1021/jacs.5b02290
J. Am. Chem. Soc. 2015, 137, 4956−4959

conductivity, enabling the realization of ultrafast rechargeable Li batteries (Figure 1b). P(NDI2OD-T2) is an electron-transporting π-conjugated polymer extensively studied in organic electronics, but only in its intrinsic and slightly n-doped states (doping level $\leq$0.1).[8] Our results demonstrate that P(NDI2OD-T2) meets key criteria for an efficient π-conjugated redox polymer: a linear π-conjugated alternating naphthalene–bithiophene backbone providing an electron-transport pathway and a naphthalene dicarboximide (NDI) unit, which is a highly reversible two-electron acceptor,[5b] ensuring a high n-doping level. The advantage of a π-conjugated redox polymer as an energy storage material over a nonconjugated one is highlighted by the design of a control polymer, poly{[*N*,*N*′-bis(2-octyldodecyl)-1,4,5,8-naphthalenedicarboximide-2,6-diyl]-*alt*-5,5′-[2,2′-(1,2-ethanyl)bithiophene]} (P(NDI2OD-TET, for synthetic details see SI)), where a saturated $-CH_2-CH_2-$ group is inserted in between the two thienyl units to break polymer backbone π-conjugation, leaving all the other P(NDI2OD-T2) structural components unaltered (Figure 1b).

The *vis-à-vis* n-dopability of the two polymers was investigated using an *in situ* electrochemical doping method. This method enables precise control of the doping process and monitoring of the property change of the polymer. Li is an ideal doping reagent because the small size of Li^+ prevents phase segregation (*vide infra*). For this purpose, coin-type rechargeable Li cells were fabricated with a polymer/conductive carbon mixture as the working electrode and metallic Li as the counter and reference electrode (see SI). Polymer/carbon black composite films containing 60 wt % of polymer with an active mass of 0.3 mg cm^{-2} was galvanostatically cycled in a Li^+-containing ethereal electrolyte solution to realize the redox process. Every NDI unit of our polymers contains four carbonyl groups, two of which are expected to be reversibly reduced via a two-step two-lithium addition reaction (Figure 2a; further

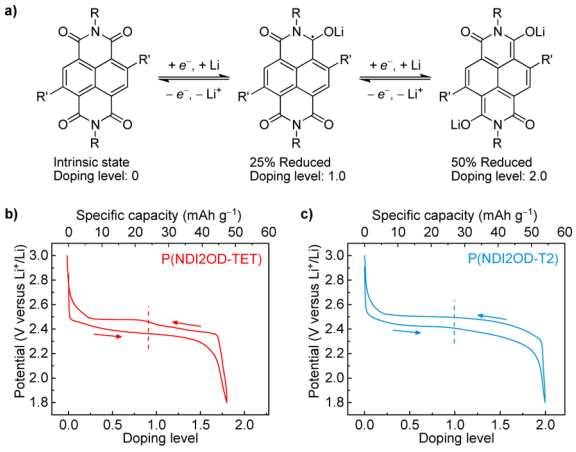

Figure 2. (a) Two-step n-doping/lithiation mechanism of the naphthalene diimide unit. (b,c) Potential profile of P(NDI2OD-TET) (b) and P(NDI2OD-T2) (c) during n-doping–undoping at 1C (2 h per cycle).

reduction of more carbonyl groups leads to irreversible transformation of the NDI structure).[9] During the two-carbonyl reduction, two electrons will be delocalized in the polymer backbone repeating units, corresponding to an n-doping level of ~2.0. Figure 2b,c shows the potential profile during the n-doping–undoping process, demonstrating that both polymers undergo two-step reduction. The two stages are less discernible for P(NDI2OD-T2), reflecting the charge delocalization by the π-conjugated backbone. Judging from the charge injected during n-doping, both polymers roughly complete the two-electron reduction, leading to high n-doping levels of 1.8 and 2.0 for P(NDI2OD-TET) and P(NDI2OD-T2), respectively. If considered as a Li storage material, the specific capacity of P(NDI2OD-T2) is 54.2 mAh g^{-1}, or 100% of its theoretical capacity (54.2 mAh g^{-1}; calculated for a 2-electron redox reaction), whereas the specific capacity of P(NDI2OD-TET) is 47.4 mAh g^{-1}, or 90% of its theoretical capacity (52.7 mAh g^{-1}). Thus, the π-conjugated backbone of P(NDI2OD-T2) does not decrease the n-dopability.

The electrode kinetics of P(NDI2OD-T2) and P(NDI2OD-TET) were compared via fast charge–discharge measurements. As shown in Figure 3a, the capacity retention at 10C (12 min

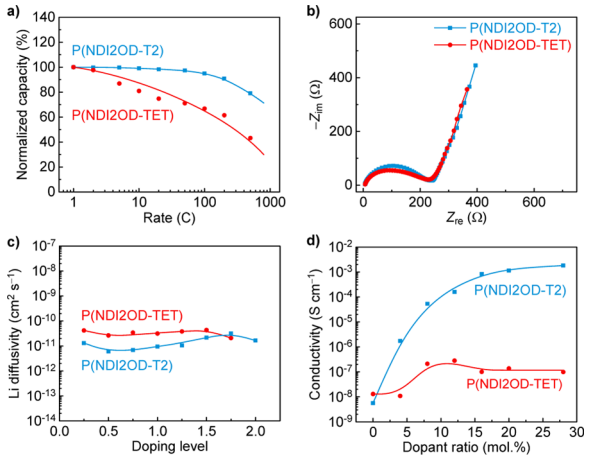

Figure 3. Electrochemical measurements for the indicated polymers. (a) Capacity retention of Li cells at increased charge–discharge rates. (b) Nyquist plot from EIS measurements of Li cells at a depth-of-discharge of 25%. (c) Solid-state Li diffusivity measured with GITT at different doping levels. (d) Electronic conductivity of polymer films without carbon additive in different chemically n-doped states.

per cycle) is 99% and 80% for P(NDI2OD-T2) and P(NDI2OD-TET), respectively, whereas at the ultrafast rate of 500C (14 s per cycle) the capacity difference between the two polymers is larger (79% and 43%, respectively). The potential difference between charge and discharge curves is also smaller for P(NDI2OD-T2) at all C-rates (Figure S1). Clearly, P(NDI2OD-T2) exhibits much faster electrode kinetics than that of P(NDI2OD-TET).

The kinetics of a solid-state battery electrode is determined by three major parameters: (1) reaction rate of the redox site, (2) solid-state ion (Li^+) transport, and (3) electronic conduction. Thus, we have measured these parameters for our polymers to understand the origin of the fast electrode kinetics of P(NDI2OD-T2). First, the redox activity was probed with electrochemical impedance spectroscopy (EIS). The obtained Nyquist plots (Figure 3b) for the two polymers at a depth-of-discharge of 25% (corresponding to a doping level of 0.5) show semicircles of about the same size in the low- to mid-frequency region, which can be fitted to yield almost identical charge transfer resistance (R_{ct} = 206.7 and 210.4 Ω for P(NDI2OD-T2) and P(NDI2OD-TET), respectively). The R_{ct} values for the two polymers remain very similar (235.5 and 223.8 Ω) at a depth-of-discharge of 75% (corresponding to a doping level of 1.5). Since R_{ct} is a measure of the

DOI: 10.1021/jacs.5b02290
J. Am. Chem. Soc. 2015, 137, 4956–4959

electrochemical reactivity of an electrode material at a given discharged state, the almost identical values indicate no obvious difference in the reaction rate for the two polymers in any n-doped state. Second, the solid-state Li diffusivity was assessed with galvanostatic intermittent titration technique (GITT), and the calculated diffusivity values are plotted against doping level (Figure 3c). The Li diffusivity−doping level dependence is similar for both polymers. The average Li diffusivities are 1.45 × 10^{-11} and 3.38 × 10^{-11} cm^2 s^{-1} for P(NDI2OD-TET) and P(NDI2OD-T2), respectively, again very close to each other. These similarities are not unexpected given the largely identical functional groups in the two polymers. The slight advantage of P(NDI2OD-TET) over P(NDI2OD-T2) in Li diffusivity may be due to the less efficient stacking of P(NDI2OD-TET) compared with P(NDI2OD-T2) (Figure S2), which allows faster Li diffusion. Finally, the film electronic conductivity of our polymers was measured for chemically doped samples. Note, conductive carbon was not used in these measurements to extract the intrinsic conductivity of the polymers. Both pristine polymers exhibit a conductivity of ∼10^{-8} S cm^{-1}. However, when reduced with progressively larger amounts of the molecular dopant 4-(1,3-dimethyl-2,3-dihydro-1*H*-benzimidazol-2-yl)-*N*,*N*-diphenylaniline (*N*-DPBI),[10] the conductivity of P(NDI2OD-T2) rapidly increases by 5 orders of magnitude to ∼10^{-3} S cm^{-1}, whereas that of P(NDI2OD-TET) only increases slightly (∼10^{-7} S cm^{-1}). These data indicate that intrachain charge transport within the π-conjugated backbone of P(NDI2OD-T2) dramatically enhances electronic conductivity, whereas that of P(NDI2OD-TET) must rely only on the less efficient interchain charge hopping. In our lithium cells, although the addition of conductive carbon will increase the apparent conductivity of the electrodes based on both polymers, the electron transport within the polymer domains will be still dominated by the intrinsic conductivity of the doped polymers. The combined results demonstrate that the presence of the π-insulating ethanyl group in P(NDI2OD-TET) does not alter the redox activity nor the ionic conductivity and that the highly conducting nature of the heavily n-doped P(NDI2OD-T2) is unambiguously responsible for the ultrafast energy storage capability.

We believe that the electronic conductivity saturation observed in Figure 3d for P(NDI2OD-T2) at *N*-DPBI molar doping ratio >15 mol % is due to inefficiencies of the dopant rather than an intrinsic limitation of the polymer. Indeed, Figure 4 compares the morphology of the pristine P(NDI2OD-T2) film, the chemically doped polymer film with 28 mol % of *N*-DPBI, and the electrochemically doped polymer film with 200 mol % of Li ion. The pristine film shows fiber-like structure as previously reported.[8a] *N*-DPBI-doped film at 28 mol % shows grainy aggregates, indicating significant phase segregation of the molecular dopant. This observation is in agreement with previous studies showing similar phase segregation of molecular dopants in the polymer host films for *N*-DPBI dopant ratio >10 mol %,[8b] thus precluding further doping. In contrast, the electrochemically Li^+-doped P(NDI2OD-T2) film exhibits negligible phase segregation and the increased surface roughness is due to the exceptionally large (200 mol %) dopant content (Figure 4c). Because of the much higher doping level, it is expected that Li-ion-doped films should exhibit similar trends but with far higher conductivities than those measured for the *N*-DPBI-doped films in Figure 3d.

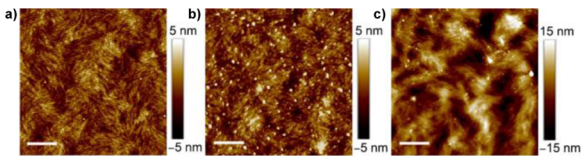

Figure 4. AFM height images of (a) pristine P(NDI2OD-T2) thin-film, (b) P(NDI2OD-T2) thin-film doped with 28 mol % of *N*-DPBI, and (c) P(NDI2OD-T2) thin-film doped with 200 mol % of Li ion. Scale bar: 500 nm. The rms roughness for three films is 1.07, 1.33, and 5.14 nm, respectively.

The improved redox kinetics of P(NDI2OD-T2) encouraged us to further explore its fast charge−discharge capability. Electrodes with higher loading (up to 1.3 mg cm^{-2}; see Figure S3) and higher active mass ratio (up to 80 wt % active mass; see Figure S4) were fabricated, and the results are compared to the state-of-the-art organic electrode materials (Table S1). For relatively "standard" high-rate conditions (∼1 mg cm^{-2}, ∼60 wt % active mass, ∼10C), very few materials approach the capacity retention level of P(NDI2OD-T2). Under more harsh testing conditions such as an ultrahigh-rate of 100C (72 s per cycle) and a high active mass ratio of ≥80 wt % (unusually high for organic electrode materials), the superiority of P(NDI2OD-T2) becomes even more evident (Table 1). Note that all these results were achieved without the need for the construction of porous polymer structures, incorporation of nanostructured 1-/2-/3-dimensional conducting reagents, or nanoscale morphology control, which are strategies usually necessary to achieve fast kinetics for organic electrode materials.[5c,11] The fact that P(NDI2OD-T2) exhibits the best electrode kinetics despite the presence of significant amount (∼57% by mass; >65% by volume from DFT computations) of redox-inactive/insulating alkyl chains in the molecular structure fully demonstrates the potential of this molecular design for energy storage purposes.

Table 1. Comparison of the Rate Capability of P(NDI2OD-T2) with Those of State-of-the-Art Electrode Materials

compound	doping type	active ratio[a]	capacity retention[b]	ref
P(NDI2OD-T2)	n	60%	95% (100C)	this work
		80%	81% (10C)	
PTCDA−PI2	n	60%	28% (80C)	12
PVK	p	55%	78% (100C)	11a
PTMA	p	50%	71% (50C)	11b
$Li_4C_6O_6$	n	80%	27% (6C)	13

[a]Only the results obtained with an active mass ratio of ≥50% and non-thin-film devices (e.g., thickness >1 μm) are included. [b]Relative to the highest capacity recorded at low rates. Only the results obtained at ≥50C (for active ratio ≥50 wt%) or ≥5C (for active ratio ≥80 wt%) are included.

The stability of P(NDI2OD-T2) when heavily n-doped and the reversibility of the doping process were investigated through repeated doping/undoping cycles. Impressively, after 3000 cycles to a doping level of 2.0 and complete undoping to the intrinsic state, the dopability of P(NDI2OD-T2) remains intact (Figure 5), with a capacity retention of 96% and an average Coulombic efficiency >99.95%. These results demonstrate for the first time that π-conjugated redox polymers can be stably and reversibly n-doped to such high levels. As a charge storage material, the specific capacity of P(NDI2OD-T2) (∼54 mAh g^{-1}) is lower than that of inorganic counterparts due to the unoptimized long solubilizing alkyl chains that do not

DOI: 10.1021/jacs.5b02290
J. Am. Chem. Soc. 2015, 137, 4956−4959

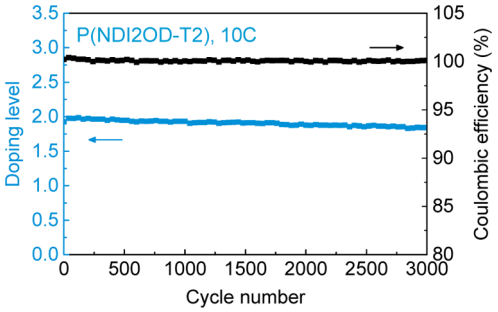

Figure 5. Reversibility of P(NDI2OD-T2) during repeated deep n-doping−undoping at 10C (12 min per cycle).

contribute to redox reaction. Thus, improved molecular design of π-conjugated redox polymers should result in significant improvement in energy density.

In summary, we have successfully demonstrated that π-conjugated redox polymers are a class of heavily n-dopable conducting polymers combining the high redox activity of redox polymers and the high electronic conductivity of π-conjugated polymers. A model polymer, P(NDI2OD-T2), was stably and reversibly n-doped to a high doping level of 2.0, a significant progress for electron-transporting π-conjugated polymers. The high electronic conductivity of the heavily n-doped P(NDI2OD-T2) leads to unprecedented electrode kinetics when evaluated as an organic electrode material for rechargeable Li batteries. With rational molecular design, π-conjugated redox polymers will establish new design space in polymer chemistry and see widespread applications especially in energy-related ones such as batteries, supercapacitors, and thermoelectrics.[14]

■ ASSOCIATED CONTENT

Supporting Information

Details on material synthesis and electrochemical measurements, detailed electrochemical measurement results. This material is available free of charge via the Internet at http://pubs.acs.org.

■ AUTHOR INFORMATION

Corresponding Authors

*yyao4@uh.edu
*afacchetti@polyera.com

Notes

The authors declare no competing financial interest.

■ ACKNOWLEDGMENTS

We acknowledge the startup funding from the University of Houston. We thank Dr. Yufeng Zhao for performing the AFM measurement for the polymer thin-film samples.

■ REFERENCES

(1) (a) Armand, M.; Tarascon, J. M. *Nature* **2008**, *451*, 652. (b) Dyer, A. L.; Bulloch, R. H.; Zhou, Y.; Kippelen, B.; Reynolds, J. R.; Zhang, F. *Adv. Mater.* **2014**, *26*, 4895. (c) Lochner, C. M.; Khan, Y.; Pierre, A.; Arias, A. C. *Nat. Commun.* **2014**, *5*, 5745. (d) Love, J. A.; Nagao, I.; Huang, Y.; Kuik, M.; Gupta, V.; Takacs, C. J.; Coughlin, J. E.; Qi, L.; van der Poll, T. S.; Kramer, E. J.; Heeger, A. J.; Nguyen, T. Q.; Bazan, G. C. *J. Am. Chem. Soc.* **2014**, *136*, 3597. (e) Yang, Y.; Chen, W.; Dou, L.; Chang, W.-H.; Duan, H.-S.; Bob, B.; Li, G.; Yang, Y. *Nat. Photonics* **2015**, *9*, 190. (f) Wu, H.; Yu, G.; Pan, L.; Liu, N.; McDowell, M. T.; Bao, Z.; Cui, Y. *Nat. Commun.* **2013**, *4*, 1943. (g) Fabiano, S.; Braun, S.; Fahlman, M.; Crispin, X.; Berggren, M. *Adv. Funct. Mater.* **2014**, *24*, 695. (h) Poizot, P.; Dolhem, F. *Energy Environ. Sci.* **2011**, *4*, 2003. (i) Song, Z.; Zhou, H. *Energy Environ. Sci.* **2013**, *6*, 2280. (j) Liang, Y.; Tao, Z.; Chen, J. *Adv. Energy Mater.* **2012**, *2*, 742.

(2) (a) Novák, P.; Müller, K.; Santhanam, K. S. V.; Haas, O. *Chem. Rev.* **1997**, *97*, 207. (b) Snook, G. A.; Kao, P.; Best, A. S. *J. Power Sources* **2011**, *196*, 1. (c) Chabinyc, M. *Nat. Mater.* **2014**, *13*, 119.

(3) (a) Mike, J. F.; Lutkenhaus, J. L. *J. Polym. Sci., Part B: Polym. Phys.* **2013**, *51*, 468. (b) Stolar, M.; Baumgartner, T. *Phys. Chem. Chem. Phys.* **2013**, *15*, 9007.

(4) (a) MacInnes, D.; Druy, M. A.; Nigrey, P. J.; Nairns, D. P.; MacDiarmid, A. G.; Heeger, A. J. *J. Chem. Soc., Chem. Commun.* **1981**, 317. (b) Wang, C. Y.; Tsekouras, G.; Wagner, P.; Gambhir, S.; Too, C. O.; Officer, D.; Wallace, G. G. *Synth. Met.* **2010**, *160*, 76. (c) Skompska, M.; Mieczkowski, J.; Holze, R.; Heinze, J. *J. Electroanal. Chem.* **2005**, *577*, 9. (d) Levi, M. D.; Gofer, Y.; Aurbach, D.; Lapkowski, M.; Vieil, E.; Serose, J. *J. Electrochem. Soc.* **2000**, *147*, 1096.

(5) (a) Häupler, B.; Burges, R.; Friebe, C.; Janoschka, T.; Schmidt, D.; Wild, A.; Schubert, U. S. *Macromol. Rapid Commun.* **2014**, *35*, 1367. (b) Song, Z.; Zhan, H.; Zhou, Y. *Angew. Chem., Int. Ed.* **2010**, *49*, 8444. (c) Song, Z.; Xu, T.; Gordin, M. L.; Jiang, Y.-B.; Bae, I.-T.; Xiao, Q.; Zhan, H.; Liu, J.; Wang, D. *Nano Lett.* **2012**, *12*, 2205. (d) Nokami, T.; Matsuo, T.; Inatomi, Y.; Hojo, N.; Tsukagoshi, T.; Yoshizawa, H.; Shimizu, A.; Kuramoto, H.; Komae, K.; Tsuyama, H.; Yoshida, J.-i. *J. Am. Chem. Soc.* **2012**, *134*, 19694. (e) Choi, W.; Harada, D.; Oyaizu, K.; Nishide, H. *J. Am. Chem. Soc.* **2011**, *133*, 19839. (f) Gao, J.; Lowe, M. A.; Conte, S.; Burkhardt, S. E.; Abruña, H. D. *Chem.—Eur. J.* **2012**, *18*, 8521. (g) Oyaizu, K.; Ando, Y.; Konishi, H.; Nishide, H. *J. Am. Chem. Soc.* **2008**, *130*, 14459. (h) Castillo-Martínez, E.; Carretero-González, J.; Armand, M. *Angew. Chem., Int. Ed.* **2014**, *53*, 5341. (i) Zhu, Z.; Hong, M.; Guo, D.; Shi, J.; Tao, Z.; Chen, J. *J. Am. Chem. Soc.* **2014**, *136*, 16461.

(6) (a) Li, Y.; Zhan, H.; Kong, L.; Zhan, C.; Zhou, Y. *Electrochem. Commun.* **2007**, *9*, 1217. (b) Levi, M. D.; Demadrille, R.; Markevich, E.; Gofer, Y.; Pron, A.; Aurbach, D. *Electrochem. Commun.* **2006**, *8*, 993. (c) Estrada, L. A.; Liu, D. Y.; Salazar, D. H.; Dyer, A. L.; Reynolds, J. R. *Macromolecules* **2012**, *45*, 8211.

(7) (a) Karlsson, C.; Huang, H.; Strømme, M.; Gogoll, A.; Sjödin, M. *J. Phys. Chem. C* **2013**, *117*, 23558. (b) Loganathan, K.; Pickup, P. G. *Electrochim. Acta* **2007**, *52*, 4685.

(8) (a) Yan, H.; Chen, Z.; Zheng, Y.; Newman, C.; Quinn, J. R.; Dotz, F.; Kastler, M.; Facchetti, A. *Nature* **2009**, *457*, 679. (b) Schlitz, R. A.; Brunetti, F. G.; Glaudell, A. M.; Miller, P. L.; Brady, M. A.; Takacs, C. J.; Hawker, C. J.; Chabinyc, M. L. *Adv. Mater.* **2014**, *26*, 2825.

(9) Liang, Y.; Zhang, P.; Chen, J. *Chem. Sci.* **2013**, *4*, 1330.

(10) Wei, P.; Oh, J. H.; Dong, G.; Bao, Z. *J. Am. Chem. Soc.* **2010**, *132*, 8852.

(11) (a) Kim, J.; Park, H.-S.; Kim, T.-H.; Yeol Kim, S.; Song, H.-K. *Phys. Chem. Chem. Phys.* **2014**, *16*, 5295. (b) Nakahara, K.; Iriyama, J.; Iwasa, S.; Suguro, M.; Satoh, M.; Cairns, E. J. *J. Power Sources* **2007**, *163*, 1110. (c) Wang, S.; Wang, L.; Zhu, Z.; Hu, Z.; Zhao, Q.; Chen, J. *Angew. Chem., Int. Ed.* **2014**, *53*, 5892. (d) Luo, C.; Huang, R.; Kevorkyants, R.; Pavanello, M.; He, H.; Wang, C. *Nano Lett.* **2014**, *14*, 1596.

(12) Wang, H.-g.; Yuan, S.; Ma, D.-l.; Huang, X.-l.; Meng, F.-l.; Zhang, X.-b. *Adv. Energy Mater.* **2014**, *4*, 1301651.

(13) Chen, H.; Armand, M.; Courty, M.; Jiang, M.; Grey, C. P.; Dolhem, F.; Tarascon, J.-M.; Poizot, P. *J. Am. Chem. Soc.* **2009**, *131*, 8984.

(14) (a) Russ, B.; Robb, M. J.; Brunetti, F. G.; Miller, P. L.; Perry, E. E.; Patel, S. N.; Ho, V.; Chang, W. B.; Urban, J. J.; Chabinyc, M. L.; Hawker, C. J.; Segalman, R. A. *Adv. Mater.* **2014**, *26*, 3473. (b) Poehler, T. O.; Katz, H. E. *Energy Environ. Sci.* **2012**, *5*, 8110. (c) Bubnova, O.; Berggren, M.; Crispin, X. *J. Am. Chem. Soc.* **2012**, *134*, 16456. (d) Bubnova, O.; Khan, Z. U.; Malti, A.; Braun, S.; Fahlman, M.; Berggren, M.; Crispin, X. *Nat. Mater.* **2011**, *10*, 429. (e) Liu, W.; Lee, J.-S.; Talapin, D. V. *J. Am. Chem. Soc.* **2013**, *135*, 1349. (f) Kim, G. H.; Shao, L.; Zhang, K.; Pipe, K. P. *Nat. Mater.* **2013**, *12*, 719.

DOI: 10.1021/jacs.5b02290
J. Am. Chem. Soc. 2015, 137, 4956−4959

Supporting Information for

Heavily n-Dopable π-Conjugated Redox Polymers withUltrafast Energy Storage Capability

Yanliang Liang,[†]Zhihua Chen,[§] Yan Jing,[†]YaoguangRong,[†] Antonio Facchetti,*[,§] Yan Yao*[,†,¶]

[†] Department of Electrical and Computer Engineering, University of Houston, Houston, Texas 77204, USA.

[§] Polyera Corporation, 8045 Lamon Avenue, Skokie, Illinois 60077, USA.

[¶]Texas Center of Superconductivity, University of Houston, Houston, Texas 77204, USA.

Experimental

Materials and general methods. P(NDI2OD-T2) was synthesized at Polyera Corp. as reported.[1] Compound **1** was synthesized according to the literature.[2]*N*-DPBIwas purchased from Sigma-Aldrich and used as is. All solvents are anhydrous grade from Sigma-Aldrich and TCI America and they were used without further purification.Unless otherwise stated, all reactionswere carried out under inert atmosphere using standard Schlenk line techniques.NMR spectra were recorded onVarian Unity Plus400 (400 MHz, room temperature) spectrometers, and chemical shifts are referenced to residual protio-solventsignals. Elemental analyses (EA) of monomers and polymer samples were performed byMidwest Microlab (Indianapolis, IN). Polymer molecular weights were determined on a Polymer LaboratoriesPL-GPC 220 using trichlorobenzene as eluent at 150 °C vs polystyrene standards.Scanning electron microscopy (SEM) was performed on a Gemini LEO 1525 microscope. Atomic force microscopy was performed on an Innova-IRIS microscopy (Bruker).

Synthesis of P(NDI2OD-TET).

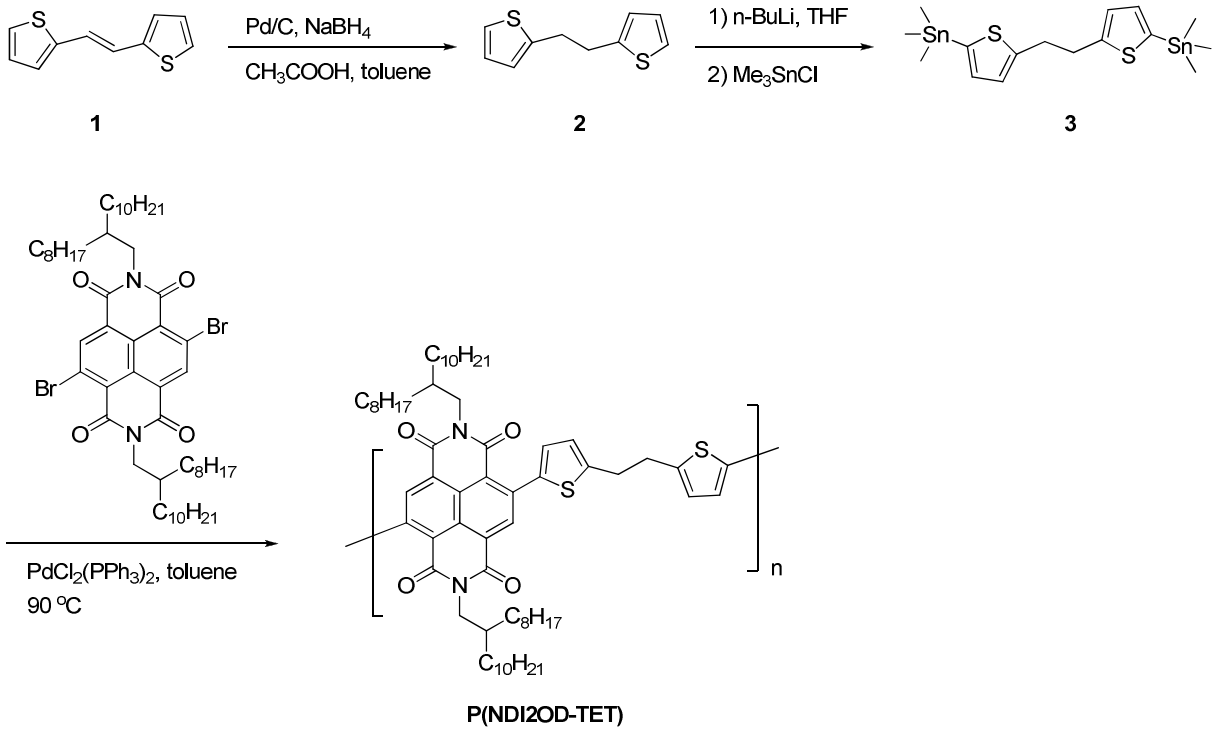

Synthesis of compound **2**: A mixture of trans-1,2-bis(2-thienyl)ethylene (compound **1**, 2.05 g, 10.66 mmol) and Pd/C (10%) (1.0 g) in toluene (50 mL) was vigorously stirred at rt, followed by addition of acetic acid (2.4 mL). Sodium borohydride (3.0 g, 79.30 mmol) was then added carefully in one portion. The resulting mixture was allowed to stir vigorously at rt for about 5 h, before it was cooled by an ice-water bath. The reaction was then quenched by addition of hydrochloride solution (0.1 M, ~10 mL). After it was basified by adding sodium hydroxide solution (1 M) to pH ~11, the mixture was filtered and the filter cake was rinsed with hexane (50 mL×2). The filtrate was then washed with water (100 mL), and the aqueous layer was further extracted by hexane (50 mL). The combined organic layer was washed with water (100 mL×2) and brine, dried over anhydrous magnesium sulfate, and concentrated in vacuo. The residue was recrystallized from methanol, leading to colorless crystals (1.19 g, 57.5%). ^{1}H NMR ($CDCl_3$, 400 MHz): δ: 7.13 (dd, J = 5.2 Hz, J = 1.2 Hz, 2H), 6.92 (dd, J = 5.2 Hz, J = 3.2 Hz, 2H), 6.80 (d, J = 3.2 Hz, 2H), 3.20 (s, 4H).

Synthesis of compound **3**: A solution of compound **2** (0.33 g, 1.70 mmol) in anhydrous THF (30 mL) was cooled to about -40 °C by an IPA/dry ice bath under argon. A solution of n-BuLi in hexane (2.5 M, 1.5 mL, 3.75 mmol) was then added slowly over a course of 15 min. The reaction was stirred at this temperature for additional 15 mins, before it was warmed to 45–50 °C and maintained for 2h. Upon cooling to –40 °C again by IPA/dry ice bath, a solution of trimethyltin chloride solution in hexane (1M, 3.8 mL, 3.80 mmol) was added slowly. The resulting reaction mixture was stirred this temperature for 30 min, before it was allowed to warm to rt and stirred at rt overnight. This reaction mixture was diluted

with ethyl ether (150 mL), washed with saturated ammonium chloride solution (100 mL× 2), dried over anhydrous sodium sulfate, and concentrated in vacuo. The residue was dried in vacuum, leading to colorless crystals (0.83 g, 93.7%), which was directly for next step without further purification. ^{1}H NMR ($CDCl_3$, 400 MHz): δ: 7.02 (d, J = 3.2 Hz, 2H), 6.95 (d, J = 3.2 Hz, 2H), 3.25 (s, 4H), 0.35 (m, 18H).

Synthesis of polymer **P(NDI2OD-TET)**: Under argon, a mixture of NDI2OD-Br_2 (0.58 g, 0.59 mmol), compound **3** (0.31 g, 0.59 mmol), and $Pd(PPh_3)_2Cl_2$ (16.5 mg, 0.024 mmol) in anhydrous toluene (35 mL) was stirred at 90 °C for 25 h. Bromobenzene (0.3 mL) was then added and the reaction mixture was maintained at 90 °C for an additional 20 h. Upon cooling to room temperature, the reaction mixture was precipitated in methanol (200 mL). The mixture was stirred at rt for 45 min, before the precipitate was collected by filtration, and washed with methanol and acetone. This crude product was then subject to Soxhlet extraction with methanol (18 h), acetone (25 h), and hexane (24 h). Finally it was extracted with chloroform (~50 mL). Upon cooling to rt, the chloroform extract was precipitated in methanol (200 mL). The precipitates were collected by filtration, washed with methanol, and dried in vacuum, leading to a red-purple solid as the product (0.49 g, 79.2%). ^{1}H NMR ($CDCl_3$, 400 MHz): δ: 8.78 (s, br, 2H) 7.20 (m, br, 2H), 6.96 (m, br, 2H),4.09 (m, br, 4H), 3.33 (m, br, 4H), 1.96 (m, br, 2H), 1.15-1.44 (m, br, 64H), 0.80-0.88 (m, br, 12H).GPC: M_n = 11.4K Da, PDI = 1.8. Elemental analysis (calc. C, 73.23; H, 8.83; N, 2.67): found C, 73.56; H, 9.11; N, 2.66.

Fabrication of electrochemical cell. For the fabrication of Li cells, composite electrodes containing P(NDI2OD-T2) and P(NDI2OD-TET) as the active materials were used as the positive electrode and metallic lithium was used as the reference and negative electrode. The polymers and Super-P carbon were hand-groundwith pestle and mortar with the aid of 1,2-dichlorobenzene without use of binders. The resulted slurry was spread onto stainless steel foil and dried at 100 °C under vacuum. For high-loading tests, the resulted films were transferred onto stainless steel mesh with mesh size of 400 × 400 and wire diameter of 0.001". CR2032 coin cells were assembled in an Ar-filled glovebox. A polypropylene membrane (Celgard) was used as the separator, and the solution of 1 M $LiClO_4$ in dioxolane–dimethoxyethane (1:1 v/v) serves as the electrolyte.

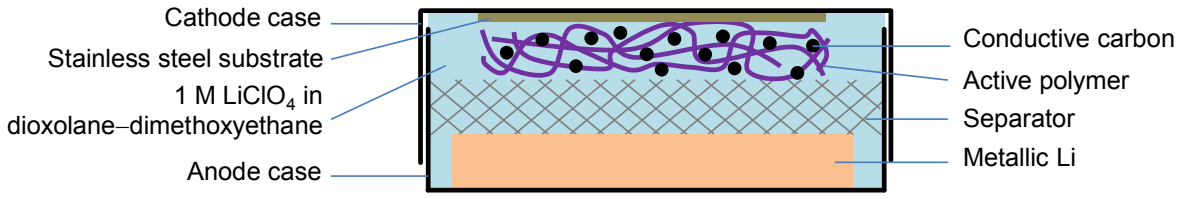

Electrochemical measurements. Electrochemical n-doping–dedoping was carried out in situ in Li cells. Charge–discharge was performed on a battery test system under galvanostatic mode (CT2001A,

LANHE). The current density at 1C is 54.2 mA g^{-1} for P(NDI2OD-T2) and 52.7 mA g^{-1} for P(NDI2OD-TET).Electrochemical impedance spectroscopy (EIS) was performed on a potentiostat (VMP3, Biologic) within 10^5–10^{-2} Hz. Cells were discharged–charged for 3 cycles and then discharged to the desired depth-of-discharge and left still for 1 h prior to measurement. Charge-transfer resistance (R_{ct}) values were fitted with a $R_s(C(R_{ct}Z_w))$equivalent circuit where R_s is the series resistance, C is a constant phase element, Z_w is the Warburg impedance.Galvanostatic intermittent titration technique (GITT) was performed with cycled cells with pulse and rest time being 15 min and 30 min, respectively, and a discharge–charge rate of C/2. Li diffusivity was calculated according to the literature.[3]

Electronic conductivity measurements. The electronic conductivity of (chemically doped) polymers films was measured using a two-probe technique on a semiconductor characterization system (4200-SCS, Keithley). All sample preparation and measurements were carried out in a N_2–filled glovebox. Solutions of 10 mM polymer and 10 m*M*-DPBI in 1,2-dichlorobenzene–chloroform (1:1 v/v) were mixed to afford the desired dopant ratio. The mixed solutions were spin-coated on glass substrates at 1000 rpm for 30 s, followed by annealing on a hotplate at 110 °C for 30 min to yield the doped polymer films. The thickness of the resulted films is 60 ± 20 nm. Ag fingers with a thickness of 100 nm were depositedonto the polymer films at a reduced pressure of 2×10^{-6} mbar.

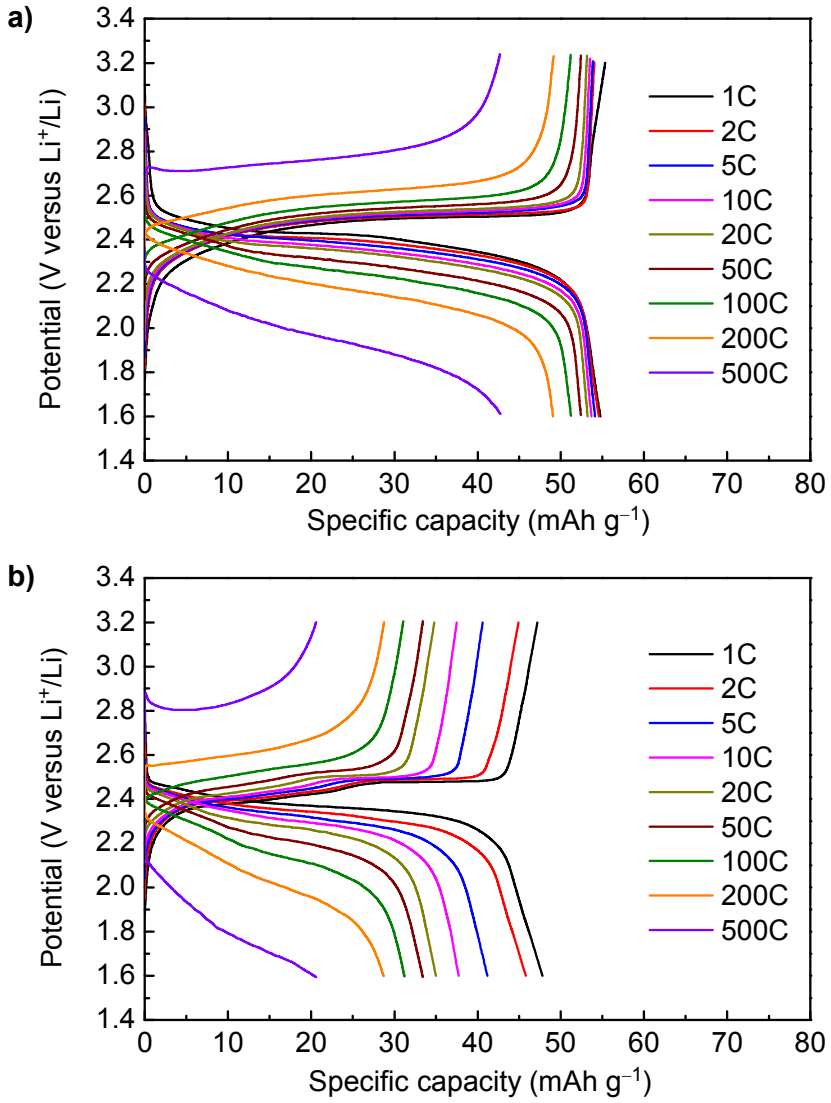

Figure S1. Charge–discharge profiles of P(NDI2OD-T2) (a) and P(NDI2OD-TET) (b) as positive electrode materials in Li cells at different charge–discharge rates. The conjugated P(NDI2OD-T2) has much better retention of both capacity and working potential than the non-conjugated P(NDI2OD-TET) as the current density increases.

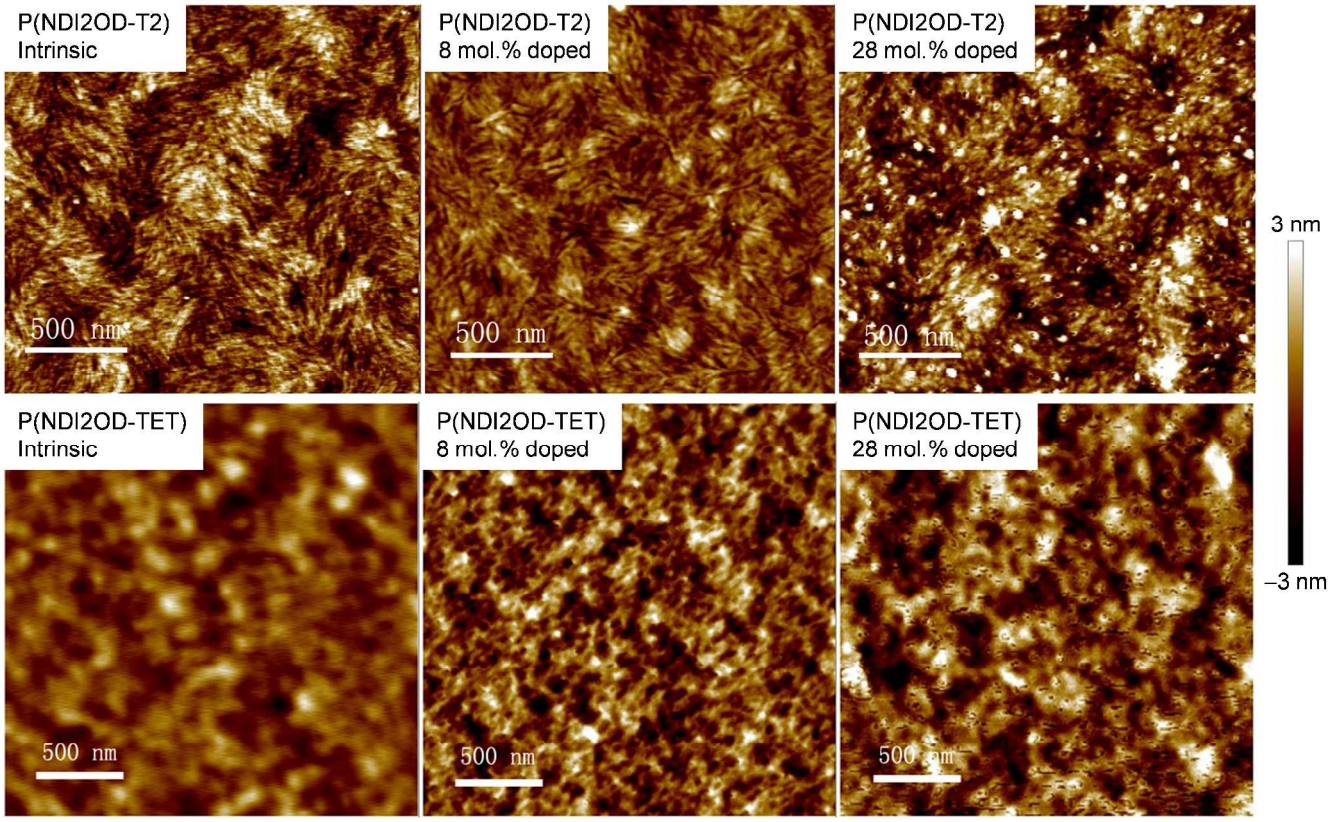

Figure S2.AFM observation of the film morphology of intrinsic and chemically doped P(NDI2OD-T2)and P(NDI2OD-TET).Both polymer show relatively uniform morphology at the intrinsic and 8 mol% doped states. At the 28 mol% doped state, aggregates form on both films, indicating phase segregation between the molecular dopant and the polymer.

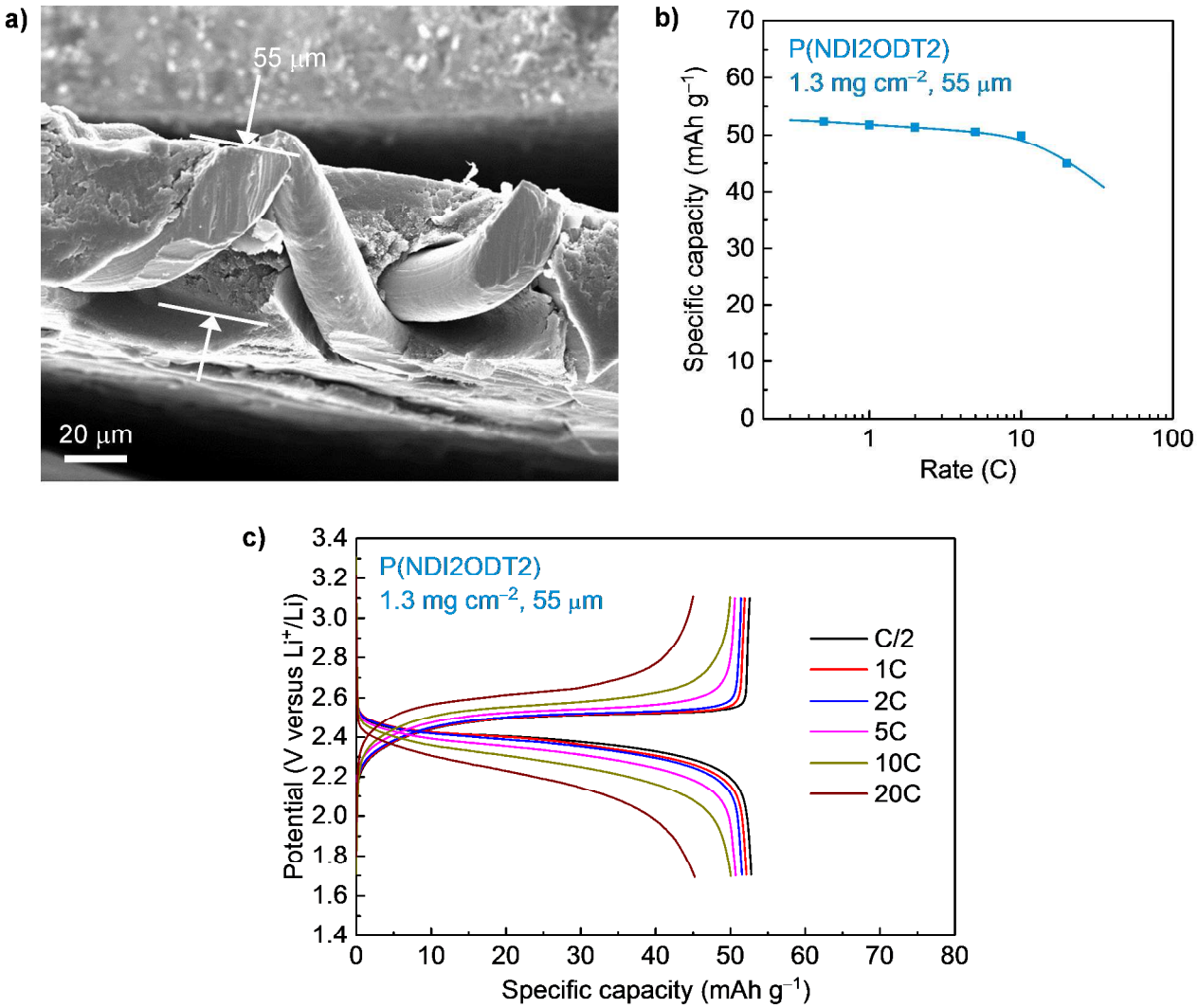

Figure S3. Investigation of P(NDI2OD-T2) electrode in high-loading conditions: the mass of active material is 1.3 mg cm^{-2}, electrode thickness is 55 μm. (a) SEM observation of the cross section of a high-loading electrode fabricated on a stainless steel mesh substrate. (b) Capacity retention of a Li cell with the high-loading electrode as the positive electrode at increasing charge–discharge rate. (c) The corresponding charge–discharge profile of the same electrode at different charge–discharge rates.

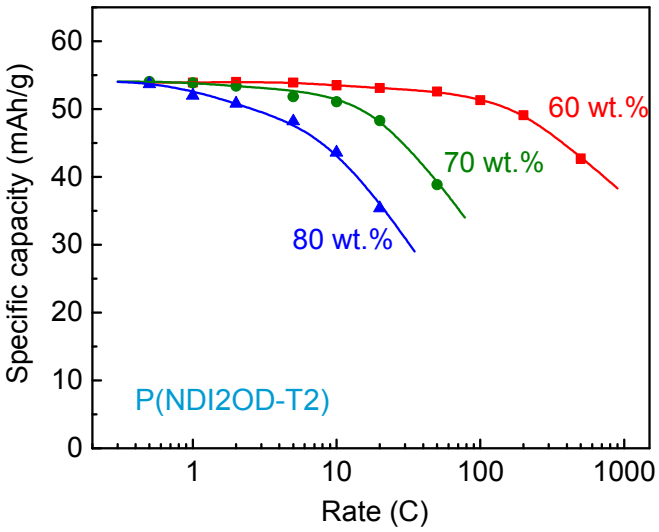

Figure S4. Performance of P(NDI2OD-T2) electrodes with a high ratio of active material in the electrode composites. The loading of active material is ca. 0.25 mg cm^{-2}.

Table S1. Comparison of the rate capability of P(NDI2OD-T2) with those of state-of-the-art organic electrode materials.

Entry	Compound	Doping type	Active ratio[a]	Active loading[b]	Capacity retention[c]	Ref.
A: Results obtained with active mass ratio at a moderate 50–70% and at high C-rates of ~10C.						
1	P(NDI2OD-T2)	n	60%	1.3 mg	95% (10C)	This work
2	Li_2PDHBQS	n	60%	1.5 mg	91% (8C)	[4]
3	PAQS@FGS	n	56%	n/a	70% (10C)	[5]
4	PI@FGS	n	53%	n/a	68% (10C)	[5]
5	Li_4-*p*-DHT	n	67%	n/a	74% (5C)	[6]
6	Li_4-*p*-DHT NS	n	59%	1.2 mg	65% (5C)	[7]
7	$Na_4C_8H_2O_6$ NR	n	65%	1.0 mg	55% (5C)	[8]
8	CADS NW	n	70%	0.6 mg	50% (6C)	[9]
9	graphene oxide	n	70%	0.4 mg	25% (5.6C)	[10]
10	PTCDA-PI2	n	60%	n/a	70% (8C)	[11]
11	HATN-CMP	n	55%	1.4 mg	33% (6.7C)	[12]
12	BFFD	n	60%	1.0 mg	78% (10C)	[13]
13	CTF BPPF	n	70%	n/a	42% (15C)	[14]
14	Na_2bpdc	n	57%	1 mg	78% (10C)	[15]
15	poly(S-TTN)	p	70%	n/a	77% (10C)	[16]
16	PTMA	p	50%	n/a	97% (10C)	[17]
17	PVK	p	50%	n/a	69% (10C)	[18]
18	PVK	p	55%	0.3 mg	95% (10C)	[19]
19	PTPAn	p	70%	n/a	90% (20C)	[20]
20	PTPAn	p	60%	n/a	92% (10C)	[21]
B: Results obtained at ultrahigh C-rates of ≥ 50C.						
21	P(NDI2OD-T2)	n	60%	0.3 mg	95% (100C)	This work
22	PTCDA-PI2	n	60%	n/a	28% (80C)	[11]
23	PVK	p	55%	0.3 mg	78% (100C)	[19]
24	PTMA	p	50%	n/a	71% (50C)	[17]
C: Results obtained with a high active mass ratio of ≥ 80 wt%.						
25	P(NDI2OD-T2)	n	80%	0.3 mg	81% (10C)	This work
26	$Li_4C_6O_6$	n	80%	n/a	27% (6C)	[22]

[a] Only the results obtained with anactive mass ratio of ≥ 50% areincluded.

[b] Only the results from non-thin-film devices (e.g. thickness > 1 μm) are included.

[c] Relative to the highest capacity recorded at low rates.Only the results obtained at ≥ 5C areincluded.

Abbriviations:

Li_2PDHBQS: poly(2,5-dihydroxy-p-benzoquinonyl sulfide)

Li_2PDHBQS: poly(2,5-dihydroxy-p-benzoquinonyl sulfide)

PAQS@GS: poly(anthraquinonyl sulfide) supported on functionalized graphene sheets

PI@FGS: poly(ethylene-naphthalenetetracarboxylicdiimide) supported on functionalized graphene sheets

Li_4-*p*-DHT (NS): dilithium (2,5-dilithium-oxy)-terephthalate (nanosheets)

$Na_4C_8H_2O_6$ (NR):tetrasodium salt of 2,5-dihydroxyterephthalic acid (nanorods)

CADS (NW): Croconic acid disodium salt (nanowires)

PTCDA-PI2: poly(ethylene-3,4,9,10-perylenetetracarboxylic diimide)

HATN-CMP:Hexaazatrinaphthaleneconjugated microporous polymers

BFFD: benzofuro[5,6-b]furan-4,8-dione

CTF BPPF: covalent triazine-based frameworks (bipolar porous polymeric frameworks)

Na_2bpdc: 4,4'-biphenyldicarboxylate sodium salts

poly(S-TTN): poly(tetrathionaphthalene-1,2,4,5-sulfide)

PTMA: poly(2,2,6,6-tetramethyl-1-piperidinyloxy-4-yl methacrylate)

PVK: poly(*N*-vinylcarbazole)

PTPAn: Polytriphenylamine

REFERENCES

(1).Chen, Z.; Zheng, Y.; Yan, H.; Facchetti, A. *J. Am. Chem. Soc.* **2008**, *131*, 8.
(2).Ngwendson, J. N.; Atemnkeng, W. N.; Schultze, C. M.; Banerjee, A. *Org. Lett.* **2006**, *8*, 4085.
(3).Weppner, W.; Huggins, R. A. *J. Electrochem. Soc.* **1977**, *124*, 1569.
(4).Song, Z.; Qian, Y.; Liu, X.; Zhang, T.; Zhu, Y.; Yu, H.; Otani, M.; Zhou, H. *Energy Environ. Sci.* **2014**, *7*, 4077.
(5).Song, Z.; Xu, T.; Gordin, M. L.; Jiang, Y.-B.; Bae, I.-T.; Xiao, Q.; Zhan, H.; Liu, J.; Wang, D. *Nano Lett.* **2012**, *12*, 2205.
(6).Renault, S.; Gottis, S.; Barres, A.-L.; Courty, M.; Chauvet, O.; Dolhem, F.; Poizot, P. *Energy Environ. Sci.* **2013**, *6*, 2124.
(7).Wang, S.; Wang, L.; Zhang, K.; Zhu, Z.; Tao, Z.; Chen, J. *Nano Lett.* **2013**, *13*, 4404.
(8).Wang, S.; Wang, L.; Zhu, Z.; Hu, Z.; Zhao, Q.; Chen, J. *Angew. Chem. Int. Ed.* **2014**, *53*, 5892.
(9).Luo, C.; Huang, R.; Kevorkyants, R.; Pavanello, M.; He, H.; Wang, C. *Nano Lett.* **2014**, *14*, 1596.
(10).Wang, D.-W.; Sun, C.; Zhou, G.; Li, F.; Wen, L.; Donose, B. C.; Lu, G. Q.; Cheng, H.-M.; Gentle, I. R. *J. Mater. Chem. A* **2013**, *1*, 3607.
(11).Wang, H.-g.; Yuan, S.; Ma, D.-l.; Huang, X.-l.; Meng, F.-l.; Zhang, X.-b. *Adv. Energy Mater.* **2014**, *4*, 1301651.
(12).Xu, F.; Chen, X.; Tang, Z.; Wu, D.; Fu, R.; Jiang, D. *Chem. Commun.* **2014**, *50*, 4788.
(13).Liang, Y.; Zhang, P.; Yang, S.; Tao, Z.; Chen, J. *Adv. Energy Mater.* **2013**, *3*, 600.
(14).Sakaushi, K.; Hosono, E.; Nickerl, G.; Zhou, H.; Kaskel, S.; Eckert, J. *J. Power Sources* **2014**, *245*, 553.
(15).Choi, A.; Kim, Y. K.; Kim, T. K.; Kwon, M.-S.; Lee, K. T.; Moon, H. R. *J. Mater. Chem. A* **2014**, *2*, 14986.
(16).Sarukawa, T.; Oyama, N. *J. Electrochem. Soc.* **2010**, *157*, F23.
(17).Nakahara, K.; Iriyama, J.; Iwasa, S.; Suguro, M.; Satoh, M.; Cairns, E. J. *J. Power Sources* **2007**, *163*, 1110.
(18).Yao, M.; Senoh, H.; Sakai, T.; Kiyobayashi, T. *J. Power Sources* **2012**, *202*, 364.
(19).Kim, J.; Park, H.-S.; Kim, T.-H.; Yeol Kim, S.; Song, H.-K. *Phys. Chem. Chem. Phys.* **2014**, *16*, 5295.
(20).Feng, J. K.; Cao, Y. L.; Ai, X. P.; Yang, H. X. *J. Power Sources* **2008**, *177*, 199.
(21).Deng, W.; Liang, X.; Wu, X.; Qian, J.; Cao, Y.; Ai, X.; Feng, J.; Yang, H. *Sci. Rep.* **2013**, *3*, 2671.
(22).Chen, H.; Armand, M.; Courty, M.; Jiang, M.; Grey, C. P.; Dolhem, F.; Tarascon, J.-M.; Poizot, P. *J. Am. Chem. Soc.* **2009**, *131*, 8984.